Journal of Cellular Biochemistry 104:965–984 (2008)

A Proteomic Study Reveals the Diversified Distribution of Plasma Membrane-Associated Proteins in Rat Hepatocytes

Xuanwen Li, Jia Cao, Qihui Jin, Chunliang Xie, Quanyuan He, Rui Cao, Jixian Xiong, Ping Chen, Xianchun Wang, and Songping Liang*

Key Laboratory of Protein Chemistry and Developmental Biology of Education Committee, College of Life Sciences, Hunan Normal University, Changsha 410081, P.R. China

Abstract To investigate the heterogeneous protein composition of highly polarized hepatocyte plasma membrane (PM), three PM-associated subfractions were obtained from freshly isolated rat hepatocytes using density gradient centrifugation. The origins of the three subfractions were determined by morphological analysis and western blotting. The proteins were subjected to either one-dimensional (1-D) SDS–PAGE or two-dimensional (2-D) benzyldimethyl-*n*-hexadecylammonium chloride (BAC)/SDS–PAGE before *nano*-Liquid Chromatography-Electrospray Ionization—tandem mass spectrometry analysis (LC-ESI-MS/MS). A total of 613 non-redundant proteins were identified, among which 371 (60.5%) proteins were classified as PM or membrane-associated proteins according to GO annotations and the literatures and 32.4% had transmembrane domains. PM proteins from microsomal portion possessed the highest percentage of transmembrane domain, about 46.5% of them containing at least one transmembrane domain. In addition to proteins known to be located at polarized liver PM regions, such as asialoglycoprotein receptor 2, desmoplakin and bile salt export pump, several proteins which had the potential to become novel subfraction-specific proteins were also identified, such as annexin a6, pannexin and radixin. Our analysis also evaluated the application of 1-D SDS–PAGE and 2-D 16-BAC/SDS–PAGE on the separation of integral membrane proteins. J. Cell. Biochem. 104: 965–984, 2008.

Key words: hepatocyte; organelle proteomics; plasma membrane; polarity; tandem mass spectrometry

Hepatocytes are highly polarized cells with their plasma membrane (PM) developed into three different morphological, biochemical, and functional types [Evans, 1980]. The sinusoidal plasma membrane (SPM), specialized for exchange of metabolites with the blood, is characterized by irregular microvilli extending into the space of Dissc and numerous coated pits; The lateral plasma membrane (LPM), which is contiguous to neighboring cell surface, is specialized for cell attachments and cell–cell communication, and thus marked by junctional complexes; The bile canalicular plasma membrane (CPM), which is separated from LPM by tight junctions, is specialized for bile secretion and characterized by numerous microvilli. A normal membrane polarity is vital for the physiological function of hepatocyte [Wang and Boyer, 2004]. Many diseases such as cholestasis, results from the lost of hepatocyte polarity [Torok et al., 1997]. Therefore, the understanding of the molecular basis under the functional membrane polarity is of significance to hepatological study.

The preparation of PM fractions originating from these three surface domains have been studied [Wisher and Evans, 1975, 1977;

This article contains supplementary material, which may be viewed at the Journal of Cellular Biochemistry website at http://www.interscience.wiley.com/jpages/0730-2312/suppmat/index.html.

Grant sponsor: National Basic Research Program of China (973 program); Grant number: 2007CB 516809; Grant sponsor: Hunan Science and Technology project; Grant numbers: 05FJ2002, 05FJ4018.

*Correspondence to: Songping Liang, Key Laboratory of Protein Chemistry and Developmental Biology of Education Committee, College of Life Sciences, Hunan Normal University, Changsha 410081, P.R. China.
E-mail: liangsp@hunnu.edu.cn

Received 13 September 2007; Accepted 3 December 2007
DOI 10.1002/jcb.21680

Evans, 1980]. Wisher et al. firstly prepared three PM subfractions including nuclear-light (N-L), nuclear-heavy (N-H), and microsomal-light (M-L) from rat liver [Wisher and Evans, 1975, 1977; Evans, 1980]. According to morphological examination and the activities of marker enzymes, they concluded that the M-L subfraction was derived predominantly from the SPM, the N-H subfraction was mainly derived from the LPM, and the CPM was present to an uncertain extent in the N-L subfraction. They further analyzed the proteins relatively enriched in three surface subfractions from liver tissue by isoelectric focusing and non-equilibrium pH gel electrophoresis followed by SDS–PAGE [Enrich et al., 1990]. However, identifying those proteins by enzyme activities and antibodies, limited the amount of membrane proteins found by this way.

Recent developments in proteomics have provided unprecedented insight into the protein composition of organelles [Wu and Yates, 2003; Durr et al., 2004; Yates et al., 2005; Gilchrist et al., 2006; Josic and Clifton, 2007], including liver PM [Zhang et al., 2005, 2006, 2007; Cao et al., 2006; Lawson et al., 2006; Ying et al., 2006]. For liver PM preparation, generally a low speed centrifugation is used to collect the nuclear fraction from the homogenate initially and PM is recovered from the nuclear fraction. As the result, these PM fragments are derived predominantly from CPM and LPM, with small amounts of SPM [Aronson and Touster, 1974; Evans, 1980]. However, SPM occupies large area of hepatocyte membrane and plays important role in the live function. Therefore, in order to clarify the overall protein composition of a liver cell surface, it is necessary to recover the whole PM fraction from different sources. Another concern in hepatocyte PM preparation is the contamination from non-hepatocyte cell. To reduce this complexity, a two-step collagenase perfusion method has been used in this study to isolate hepatocytes. Most importantly, the polarity is maintained during the perfusion process [Wisher and Evans, 1977].

In the present study, by using three different PM-associated subfractions from freshly isolated rat hepatocytes, we aimed to determine the proteins compositions of the three subfractions by proteomic approaches. At the same time, we explored the feasibility to ascribe the proteins revealed by proteomics research to distinct PM-associated regions and polarity-related functions.

EXPERIMENTAL

Materials

Electrophoresis grade chemicals were obtained from GE Healthcare (Uppsala, Sweden) or Bio-Rad Laboratories (Hercules, CA). Anti-prohibitin monoclonal antibody, anti-flotillin monoclonal antibody, anti-Golgi 58 monoclonal antibody, and horseradish peroxidase-conjugated anti-mouse IgG were obtained from BD Bioscience (San Jose, CA). Anti-GRP 94 monoclonal was from Stressgen (Stressgen Biotechnologies, Victoria, BC, Canada), anti-Na^+/K^+ ATPase monoclonal antibody were purchased from Abcam (Cambridge, UK); Adenylyl cyclase V/VI and 5m′-nucleotidase were from Santa Cruz biotechnology (Santa Cruz, Canada). Benzyldimethyl-*n*-hexadecylammonium chloride (16-BAC) and all other chemicals (analytical grade) were from Sigma (St. Louis, MO) unless specified. Rats (200–250 g) were purchased from CentreSouth University (Changsha, China).

Isolation and Purification of Rat Hepatocytes

Hepatocytes were isolated and purified by the two-step procedure of Seglen [1976] with minor modifications. Briefly, the rats were starved for 16 h before anesthesia with 10% chloral hydrate. In the first stage, the liver was perfused via the portal vein with wash-out medium consisting of Hank's saline solution (HBSS pH 7.2, lacking calcium and magnesium) buffered with 15 mM HEPES and supplemented with 0.02% EDTA to remove blood cells. In the second stage, the connective tissue in the liver was disrupted by perfusion with complete HBSS buffered with 15 mM HEPES and supplemented with 0.45 mg/ml collagenase. After perfusion, the hepatocytes were gently removed from the biliary tree by mechanical disruption and filtered twice through a 40 μm nylon mesh. Viable hepatocytes were enriched by low-speed centrifugation at 50 g for 3 min twice to remove non-hepatocytes.

Isolation of Hepatocyte PM-Associated Subfractions

The procedure was modified from the previous work [Fleischer and Kervina, 1974;

Wisher and Evans, 1975, 1977]. Firstly, the cells were suspended in ice-cold isotonic homogenization buffer (0.25 M sucrose, 5 mM Tris–HCl, with complete protease inhibitor cocktail, pH 7.6) and homogenized firstly in a Dounce homogenizer with a loose-fitting pestle for five passes and secondly then using a hand-held disperser (IKA products, T8 ULTRA-TURRAX, Germany) until more than 90% of the hepatocytes were disrupted as confirmed by the Trypan Blue exclusion method [Tennant, 1964]. The homogenate was centrifuged at 1,000*g* for 10 min at 4°C, and the pellet was resuspended in the same initial homogenization with one up-and-down stroke of the loose pestle. The nuclear fraction was separated as before, and the supernatant were combined. Re-homogenization and re-centrifugation of the nuclear pellet were performed a third time. All the homogenization process was produced at 4°C. In order to obtain a microsomal pellet, the combined supernatant solutions were centrifuged at 33,000*g* for 8 min at 4°C, and the supernatant was then centrifuged at 78,000*g* for 100 min at 4°C. The nuclear and the microsomal fraction were used for the next PM subfractions purification. Both fractions were then thoroughly mixed with 60% sucrose to achieve a density at least 49%. After centrifugation at 10,000*g* for 12 h at 4°C, two PM-associated subfractions derived from the nuclear fraction were obtained at sucrose density interface of 8–37% (w/w) named N-L and 37–40% (w/w) named N-H, and one from the microsomal fraction was collected at sucrose density interface of 8–34% (w/w) named M-L. Finally, aliquots of the three subfractions were fixed with 2.5% glutaraldehyde for the subsequent transmission electron microscopy (TEM) [Zhang et al., 2006], and the rest was then stored in the homogenization buffer at −80°C for the next analysis.

SDS–PAGE and Western Blotting Analysis

To examine the purity of the subfractions using western blotting, different samples were dissolved directly in 2% SDS sample buffer. For the protein separation and the subsequent identification, the three subfractions from sucrose density centrifugation were firstly diluted 200 times with 0.1 M Na_2CO_3 (pH 11), kept on ice for 30 min and centrifuged at 18,000*g* for 30 min at 4°C. The supernatant was concentrated and desalted using Centriplus centrifugal concentrators (YM-3, MWCO 3 kDa; Millipore) according to the manufacture's protocol. The supernatant and the pellet from the Na_2CO_3 treatment were saved and solubilized in 2% SDS sample buffer for the subsequent analysis. After determining the protein concentration with the Bio-rad RC DC™ Protein Assay kit (Bio-Rad), the samples were subjected to SDS–PAGE using 11.5% separation gel and 4.8% stacking gel. The gel was stained using Coomassie Brilliant Blue G250 for the subsequent Mass spectrometry analysis. For western blotting analysis, the proteins in the gel were transferred to a PVDF membrane and performed as described before [Cao et al., 2006; Chen et al., 2006].

16-BAC/SDS–PAGE Analysis

The Na_2CO_3-washed pellet was incubated at 60°C for 5 min in BAC sample buffer [6 M urea, 55 mM DTT, 7.5% (w/v) 16-BAC, 5% glycerol (w/v), 0.05% (w/v) Pyronin Y]. After visualization with Coomassie G-250 solution, the first dimension gel strip was equilibrated in reducing and alkylating solutions as described [Hartinger et al., 1996]. The pH-adjusted strips were placed on the top of an 11.5% SDS–PAGE gel. After running the second dimension, the gels were stained with Coomassie G-250.

In-Gel Digestion and Mass Spectrometry Analysis

Both the gel lanes from the 1-D SDS–PAGE and the gel spots from the 16-BAC/SDS–PAGE were selected for the tandem mass spectrometric analysis. The in-gel digestion was done according to our previous work [Cao et al., 2006; Chen et al., 2006; Zhang et al., 2007]. The final solution was lyophilized in a SpeedVac to about 3 μl.

The digested peptides were injected into a capillary LC system (Waters) and first desalted and preconcentrated on a pre-column (C18 PepMap™, 0.3 mm i.d., 5 mm length, LC Packings). The peptides were then eluted onto a C18 column (C18,75 μm i.d.,15 cm length, LC Packings) coupled to a quadrupole time-of-flight (Q-TOF) microhybrid mass spectrometer (Q-TOF micro™, Waters, Micromass, Manchester, UK) using a Micromass *nano*-ESI source. The gradient profile consisted of a linear gradient from 5% B (0.1% formic acid/4.9% H_2O/90% acetonitrile, v/v) to 50% B in 65 min followed by 85% B for 10 min, then the column was reconditioned with 95% A (0.1% formic acid/4.9% acetonitrile/95% H_2O, v/v) solution for 10 min. The flow rate was 200 nl/min. The

peptides were detected in the positive ion MS mode or the data-depend MS/MS mode. Data-depend mode was conducted using survey scans (m/z 400–1,400) to choose the three most intense precursor ions (with charge states ≥ 2) for a collision-induced dissociation (CID). The collision energies were chosen automatically as a function of m/z and charge. The collision gas was argon. The temperature of the heated sample source was 85°C and the electrospray voltage was 3,000 V.

Data Processing and Bioinformatics Analysis

The tandem mass spectrometry (MS/MS) data were acquired and converted to PKL files by the software MassLynx (Micromass). The PKL files, which consist of the mass values of the precursor ions and the intensity and the mass values of the fragment ions, were analyzed using MASCOT software (www.matrixscience.com). Search parameters were set as following: the International Protein Index (IPI) rat database (version 3.07, www.ebi.ac.uk/ipi, 39,441 entries); trypsin enzyme, allowing up to one missed cleavage; peptide mass tolerance was 0.6 Da and MS/MS mass tolerance was 0.3 Da; fixed modification parameter was carbamidomethylation, and the variable modification parameter was oxidation (Met). We selected candidate peptides with probability-based Mowse scores (total score) that exceeded their threshold, indicating a significant (or extensive) homology ($P < 0.05$), and referred to them as "hits" [Cao et al., 2006; Zhang et al., 2007]. Proteins that were identified with at least two peptides showing both a score higher than 34, were validated without any manual validation. For proteins identified by only one peptide having a score higher than 34, the peptide sequence was systematically checked manually to confirm or cancel the MASCOT suggestion. For the positive identification, the assignment had to be based on four or more consecutive y- or b-series ions (e.g., y4, y5, y6, y7). To calculate confidence levels and false positive rates, a decoy database containing the reverse sequences of all the proteins in the target component was appended to the rat database. The MS/MS data were then searched against the combined forward/reverse database.

A Perl script was written in house to parse significant hits from Mascot output files (html files) into tab delimited data files suitable for subsequent data analysis. An automated sequence retrieval script was written in Perl using the Bioperl libraries to generate a FASTA formatted protein sequence from IPI databases for proteins identified by each MS experiment. The molecular mass values, pI values and the number of peptides used to identify a protein as well as the sequence and charge state of each peptide were retrieved from Mascot output files. The average hydropathy for identified proteins was calculated using the ProtParam software available at http://us.expasy.org by submitting each FASTA file in batch. The proteins exhibiting positive GRAVY values were recognized as hydrophobic and those with negative values were deemed hydrophilic. Protein abundance estimates were determined using exponentially modified protein abundance index (emPAI) values [Ishihama et al., 2005]. When a protein was identified for several times, only the protein with the highest Mascot score was taken into consideration. The subcellular location and function of the identified proteins were elucidated by gene ontology (GO) cellular component and function terms, respectively. The mapping of putative transmembrane domains was carried out using the transmembrane hidden Markov model (TMHMM v 2.0) algorithm, available at http://www.cbs.dtu.dk/services/tmhmm.

RESULTS

Isolation of Three PM-Associated Subfractions From Perfused Hepatocytes

Liver tissue is composed of parenchymal, hepatocyte, and non-parenchymal cells. To reduce proteome complexity and favor the identification of low abundance proteins, hepatocytes prepared by collagenase perfusion have been used in this study. The strategy for isolation and analysis of the hepatocyte PM-associated subfractions is shown in Figure 1. The typical yield of isolated hepatocytes was about 10^7 cells per gram liver tissue and cell viability was greater than 90% as assessed by the Trypan Blue exclusion method. The hepatocyte purity checked by phase-contrast microscopy was over 95% (data not shown). The overall recovery was about 10.3 mg PM/g liver, including 2.5 mg from N-L, 2.1 mg from N-H, and 5.7 mg from M-L fraction.

Characterization of three PM-associated subfractions was determined by TEM firstly (Fig. 2). Consistent with the previous work, the N-L subfraction presented a specific profile,

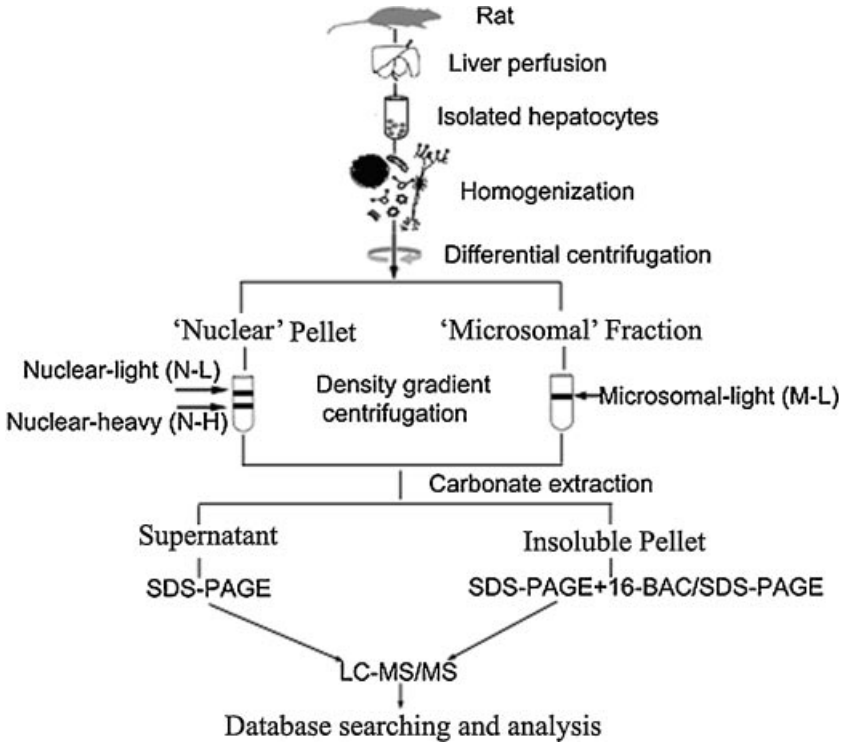

Fig. 1. Schematic methodology for the proteomic analysis of PM-associated subfractions from rat hepatocytes.

multiple small vesicles encircled by a giant encircling membrane (Fig. 2A) [Hubbard et al., 1983]. The N-H subfraction was characterized by the presence of membrane strips and junctional complexes as indicated in Figure 2B. The magnified insert showed the typical junctional structures. M-L subfraction was mainly composed of irregular vesicles (Fig. 2C) as described before [Hubbard et al., 1983]. Further identification was performed by western blotting against the specific protein markers (as shown in Fig. 3): Firstly, as the marker of universal PM fractions in Figure 3A, flotillin signals were enhanced dramatically in all three PM-associated subfractions, indicating the enrichment of PM after preparation. It also showed that N-L was the highest one, almost 20-fold compared with crude homogenates, when N-H fraction exhibited much weaker signal. Na^+-K^+ ATPase, an important marker for basolateral PM fraction showed very strong signal in the M-L subfraction when N-L and N-H fractions exhibited weak signal. Adenylyl cyclases V/VI, a blood-sinusoidal marker protein, showed the

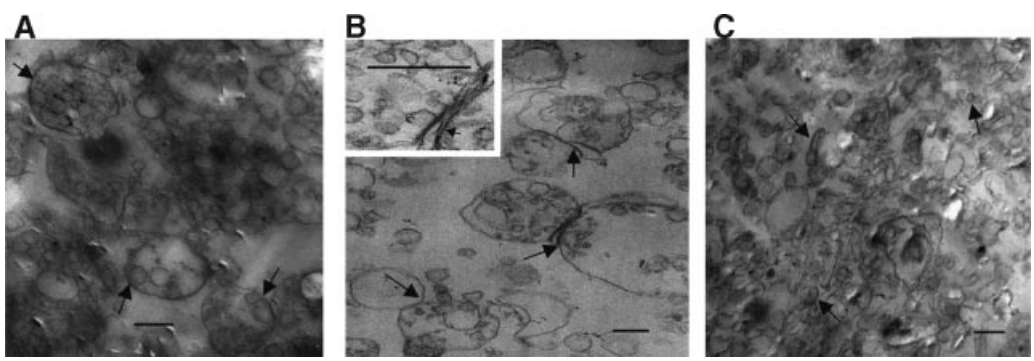

Fig. 2. Characterization of the three subfractions by transmission electron microscopy. **A**: The N-L subfraction; (**B**) the N-H subfraction, the insert indicates the amplified structure of straight segments of two parallel membranes; (**C**) the M-L subfraction. The arrows show the representative structures in each subfraction. The bars represent 0.5 μm.

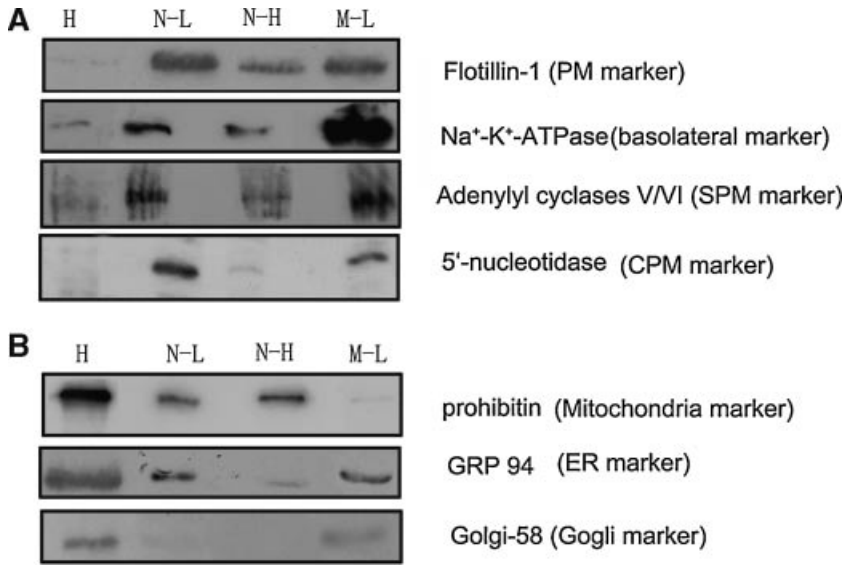

Fig. 3. The purities of the three subfractions were determined using western blotting against special subcellular protein markers. The same protein amount was loaded on each lane. The representative pictures were shown here from three replications. **A**: Western blotting against PM markers. **B**: Western blotting against intracellular organelle markers. H, total hepatocyte homogenate; N-L, the proteins from N-L subfraction; N-H, the proteins from N-H subfraction; M-L, the proteins from M-L subfraction.

highest abundance in the M-L subfraction. Additionally, this signal in M-L subfraction was enriched over 20-fold compared with the homogenates. N-L subfraction showed the strongest signal for 5′-Nucleotidase, a CPM marker protein concentrated at the bile canaliculus [Wachstein and Meisel, 1957], which is over 20-fold relative to the crude homogenates.

Except for integrity, the sample purity is another important factor in organelle proteomic analysis. In all three fractions as shown in Figure 3B, the signals of prohibitin (as mitochondria marker protein), Golgi 58 (as Golgi marker protein), GRP 94 [as endoplasmic reticulum (ER) marker protein] decreased obviously after purification, but to different extent, respectively. The N-L subfraction was mainly contaminated from mitochondria and ER, which had few contaminations from Golgi. The N-H subfraction had contaminations mainly from mitochondria and had few contaminations from ER and Golgi. The M-L had the most contaminations from Golgi, and the ER contaminations were the same as the N-L subfraction. However, this subfraction had almost no contaminations from mitochondria. Therefore, we reasoned that our prepared subfractions represented a good sample source for the proteomic analysis of the PM-associated proteins of hepatocytes.

Evaluation of the Effect of Na_2CO_3 Treatment

Na_2CO_3 treatment has been frequently used for the extraction of peripheral and membrane-associated proteins. However, the proteins recovered from the supernatant have not been given enough attention. In this study, we included the supernatant fraction to get a comprehensive understanding of the hepatocyte PM composition. After extraction with 0.1 M Na_2CO_3 and subsequent centrifugation at 18,000*g* for 30 min as described before [Millar and Heazlewood, 2003; Marmagne et al., 2004; Zhang et al., 2005, 2006], the supernatant and the pellet were separated by 1-D SDS–PAGE. As shown in Figure 4A,B, the staining patterns

Fig. 4. Separation patterns of the three PM-associated subfraction on 1-D SDS–PAGE. The same protein amount was loaded on each lane or gel. The molecular markers were shown on the left. **A**: The proteins from the supernatant of Na_2CO_3 treatment were separated by 1-D SDS–PAGE; (**B**) the proteins from the pellet of Na_2CO_3 treatment were separated by 1-D SDS–PAGE; (**C**) the overlap of the proteins from supernatant and pellet after Na_2CO_3 treatment only separated using 1-D SDS–PAGE; (**D**) the theoretical pI distribution of the proteins from supernatant and pellet after Na_2CO_3 treatment separated using 1-D SDS–PAGE, 1 D-SDS meant all the proteins identified from the 1-D SDS–PAGE; (**E**) the number of predicted helices distribution of the proteins from supernatant and pellet after Na_2CO_3 treatment separated using 1-D SDS–PAGE, 1 D-SDS meant all the proteins identified from the 1-D SDS–PAGE. The bars indicate the percentage of proteins.

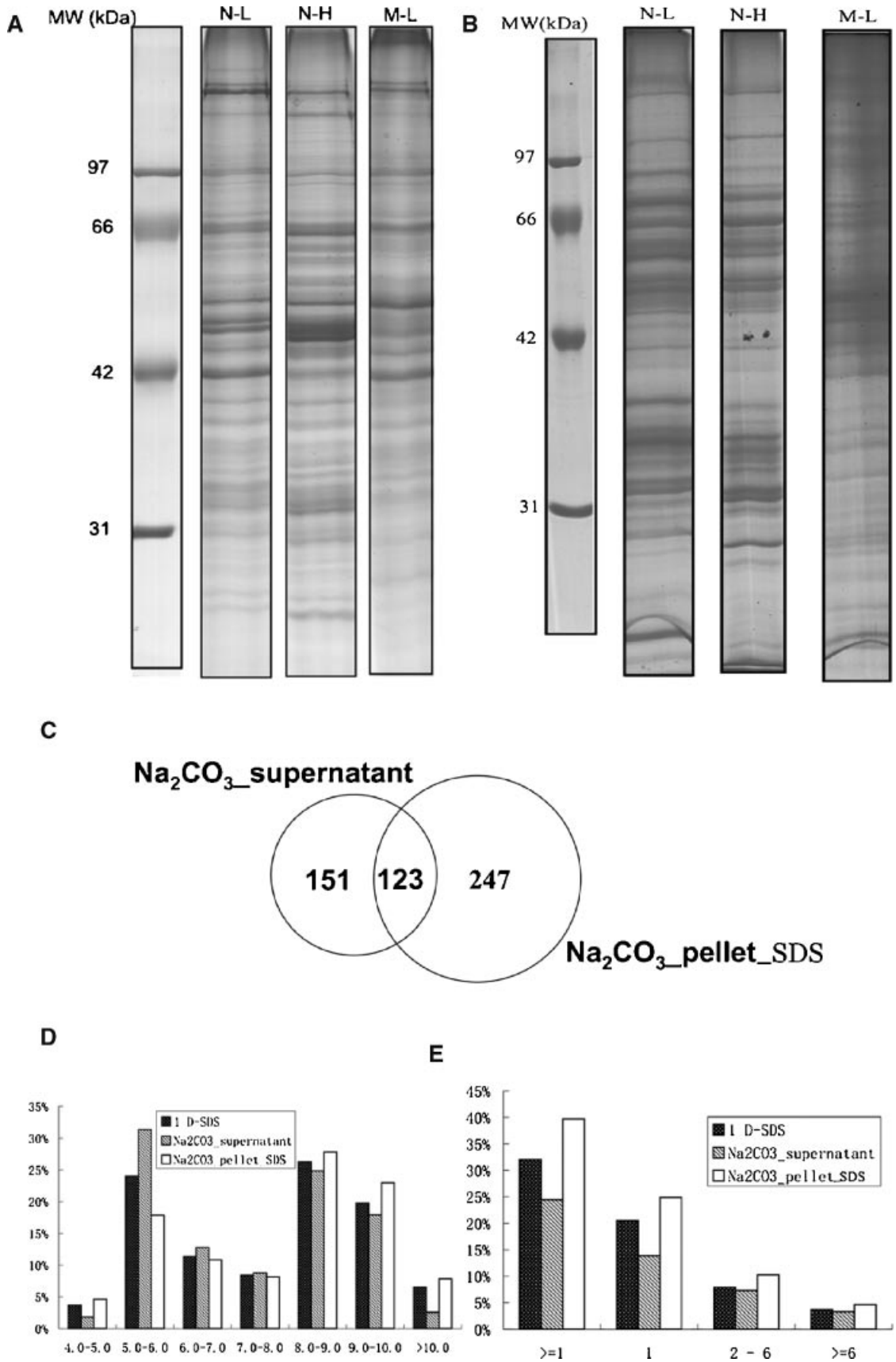
A
MW (kDa)
N-L
N-H
M-L
97
66
42
31
B
MW(kDa)
N-L
N-H
M-L
97
66
42
31
C
Na2CO3_supernatant
151
123
247
Na2CO3_pellet_SDS
D
1 D-SDS
Na2C03_supernatant
Na2C03_pellet_SDS
35%
30%
25%
20%
15%
10%
5%
0%
4.0-5.0
5.0-6.0
6.0-7.0
7.0-8.0
8.0-9.0
9.0-10.0
>10.0
E
1 D-SDS
Na2C03_supernatant
Na2C03_pellet_SDS
45%
40%
35%
30%
25%
20%
15%
10%
5%
0%
>=1
1
2 - 6
>=6

Fig. 4.

were similar, but intensities of some bands were different. The overlap of identified proteins from the supernatant and the pellet fractions was shown in Figure 4C.

To understanding the analytical bias of the Na_2CO_3 treatment, the identified proteins from the supernatant and the pellet of N-L, N-H, and M-L using the 1-D SDS–PAGE strategy were classified according to four physicochemical index, molecular weight (MW), pI value, and hydrophobicity (Fig. 4D,E and Supplementary Fig. S1). With view to the MW and hydrophobicity character, the percentage of hydrophobic proteins in the pellet and the supernatant were similar (Supplementary Fig. S1A,S1B). While the pellet fraction showed advantages for alkaline proteins ($pI > 9$) as indicated in Figure 4D, which was consistent with our previous work [Zhang et al., 2006]. According to the TM prediction by TMHMM, 39.7% of the proteins from the pellet fraction were transmembrane proteins. However, there was 24.5% of the supernatant fraction had at least one transmembrane domain (Fig. 4E), which even higher than our previous data on the liver tissue [Zhang et al., 2006]. Most importantly, a few important functional proteins located in hepatocyte PM were only identified in the supernatant fraction. Solute carrier organic anion transporter (IPI00231882), which confined to the basolateral PM of hepatocytes and mediates the Na^+-independent transport of organic anions such as taurochlate, bromosulfophthalein and steroid conjugates, was identified only from the supernatant fraction. Similar to lerk-5 (IPI00365395), which is one of the erythropoietin-producing hepatocellular (EPH)-related receptor kinase ligand and plays important roles in controlling cell localization and organization, was also only identified from the supernatant fraction.

Membrane Protein Separation With 16-BAC/SDS–PAGE and 1-D SDS–PAGE

Traditionally, 2-DE employing IEF as the first dimension encounters limitations in the separation of membrane proteins for the use of mild non-ionic detergents and extremely low concentrations of salt ions [Wu and Yates, 2003]. The 1-D SDS–PAGE or an improved 2-DE using ionic detergent, such as 16-BAC, CTAB, or SDS as another dimension were especially designed for a comprehensive membrane proteome research [Hartinger et al., 1996; Wu and Yates, 2003; Josic and Clifton, 2007]. We firstly used the 1-D SDS–PAGE to separate the membrane proteins before the LC-MS/MS (Fig. 4B). In order to increase the protein separation resolution of the most interesting fractions from the alkaline-treated pellet and get more information for the abundance of some single protein, 16-BAC/SDS–PAGE was further used to separate the alkaline-treated pellet (Fig. 5A–C). As expected, by focusing the proteins into localized spots, 16-BAC/SDS–PAGE had an obvious improvement on the sensitivity of protein identification. The overlap of proteins using the two separation methods was shown in Figure 5D. There are 92 proteins which were identified only from the 16-BAC/SDS–PAGE, which may indicate their low abundance expression in hepatocyte PM, including Ras GTPase-activating protein syngap (IPI00339023) with an emPAI value of 0.02, syndapin iii (IPI00199145), a large GTPase dynamin interacting protein [Kessels and Qualmann, 2004] with an emPAI value of 0.02. As expected, 16-BAC/SDS–PAGE and the 1-D SDS–PAGE had no distinct differences in the GRAVY value and the TM number (Supplementary Fig. S1C,S1D). Such as nicotinamide nucleotide transhydrogenase (IPI00555265) having 12 TM regions and solute carrier organic anion transporter family, member 1A4 (IPI00214031) having 11 TM were still separated effectively using the 16-BAC/SDS–PAGE. 16-BAC/SDS–PAGE even showed its advantages in separating alkaline proteins ($pI > 9$) as indicated in Figure 5E. However, 16-BAC/SDS–PAGE and the 1-D SDS–PAGE have quite different priority on the MW of proteins (Fig. 5F). It is difficult for 16-BAC/SDS–PAGE to separate proteins with high MW, especially those higher than 200 kDa [Morciano et al., 2005; Burre et al., 2007]. This may be the intrinsic defect of 2-D electrophoresis, including the traditional IEF/SDS–PAGE.

Hepatocyte PM-Associated Proteome With Partial Subfraction Information

Using the stringent criteria mentioned above, 613 non-redundant proteins were identified, with 416, 307, and 221 proteins from the N-L, N-H, and M-L fractions, respectively (Supplementary Table S1). The overlap proteins of

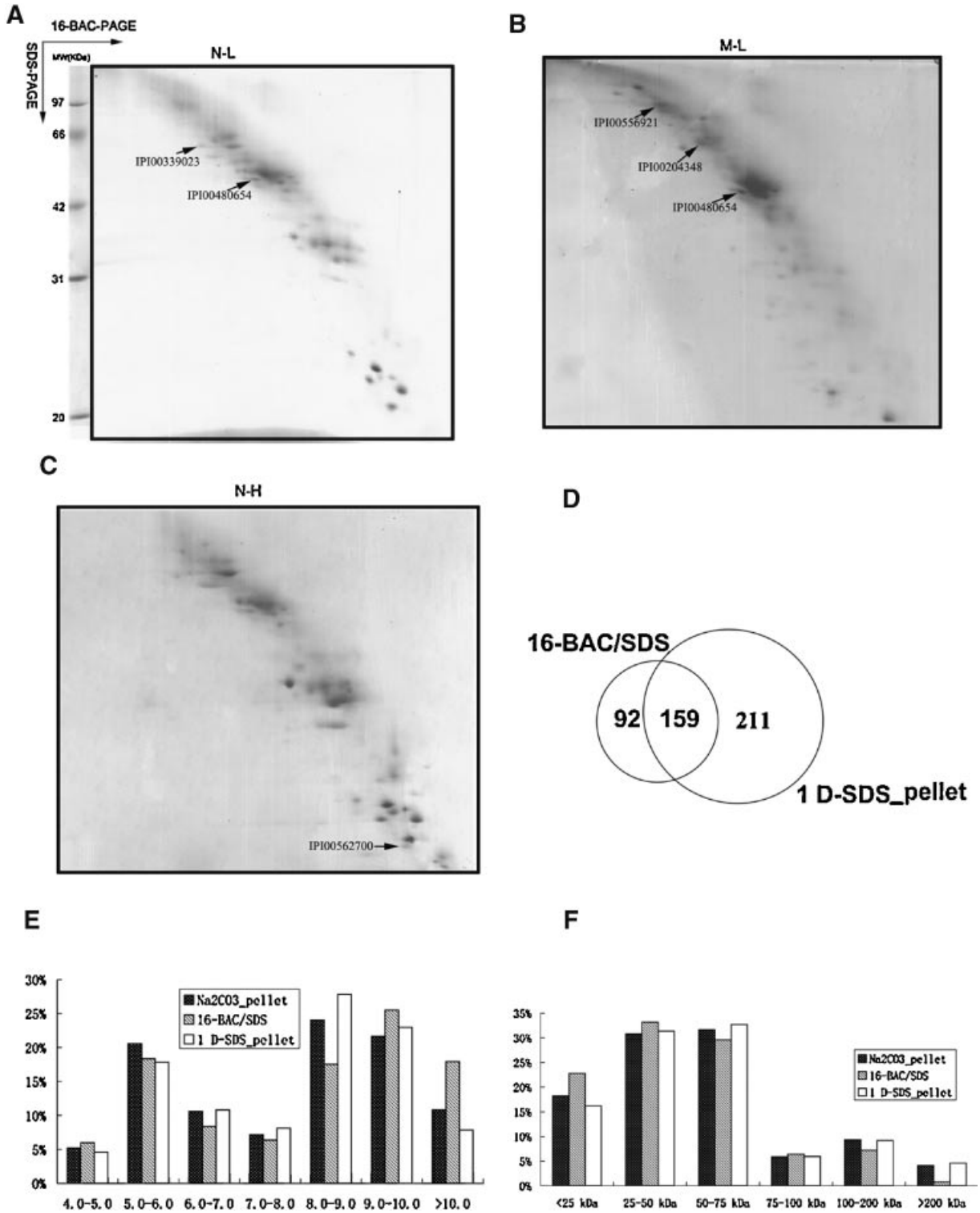

Fig. 5. Two-dimensional separations of proteins from pellet of PM-associated subfractions after Na_2CO_3 treatment by 16-BAC/SDS–PAGE. The same protein amount was loaded on each lane or gel. The molecular markers were shown on the left. The arrows point to some proteins which were not identified from 1-D SDS–PAGE. **A**: N-L subfraction; (**B**) M-L subfraction; (**C**) N-H subfraction; (**D**) the overlap of the proteins from the pellet after Na_2CO_3 treatment separated using both 1-D SDS–PAGE and 16-BAC/SDS–PAGE; (**E**) the theoretical pI distribution of the proteins from the pellet after Na_2CO_3 treatment separated by 1-D SDS–PAGE and 16-BAC/SDS–PAGE, Na2CO3_pellet meant all the protein identified from pellet after Na_2CO_3 treatment; (**F**) the theoretical mass distribution of the proteins from the pellet after Na_2CO_3 treatment separated by 1-D SDS–PAGE and 16-BAC/SDS–PAGE, Na2CO3_pellet meant all the protein identified from pellet after Na_2CO_3 treatment. The bars indicate the percentage of proteins.

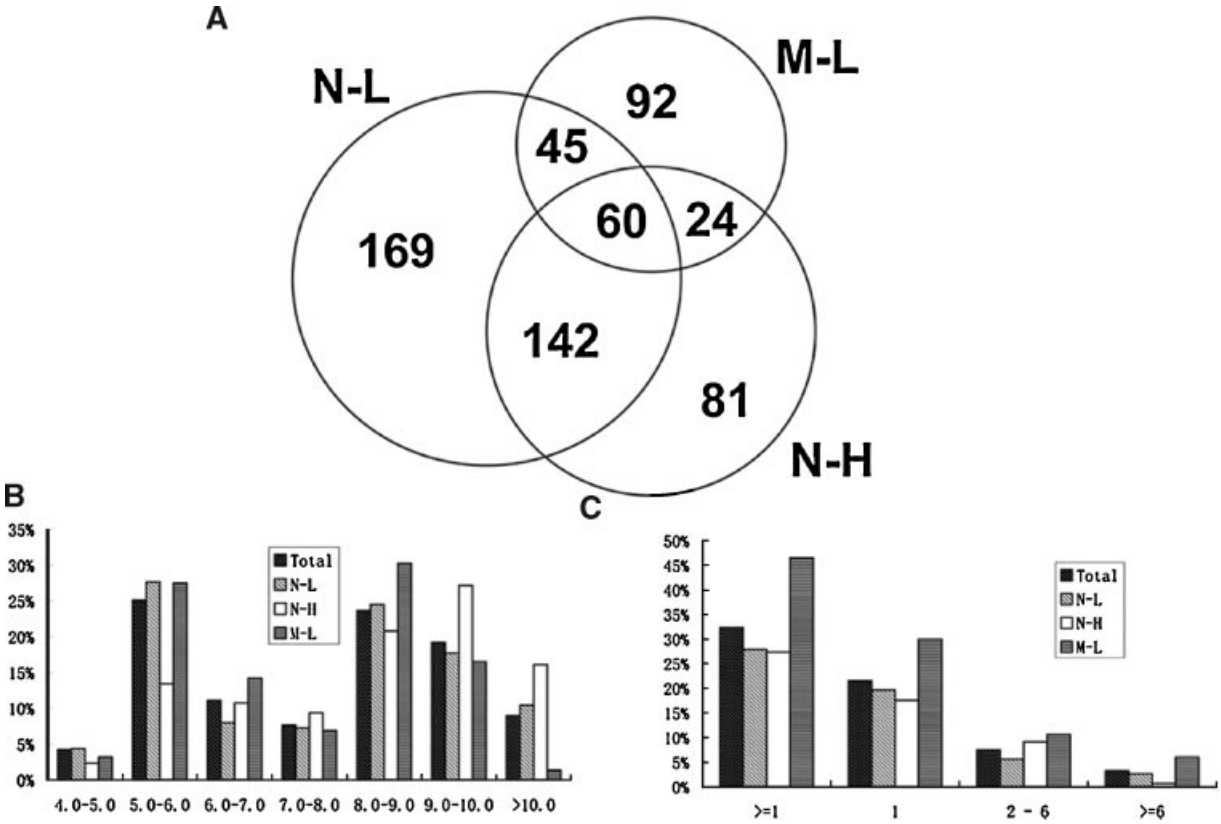

Fig. 6. **A**: Schematic diagram showing the overlap of proteins identified from different subfractions; (**B**) the theoretical pI distribution of the proteins from the three subfractions; (**C**) the number of predicted helices distribution of the proteins from the three subfractions. Total meant all the proteins identified, N-L meant all the proteins identified from the N-L subfractions, N-H meant all the proteins identified from the N-H subfractions, M-L meant all the proteins identified from the M-L subfractioons. The bars indicate the percentage of proteins in each.

different subfractions were shown in Figure 6A. The estimated false positive rate of protein identification was 4.3% through searching the combined forward/reverse database.

According to physicochemical properties, proteins from three subfractions showed relatively similar distribution pattern (Fig. 6 and Supplementary Fig. S1), except for those from N-H subfraction, which had a few more proteins with lower MW and higher pI (Fig. 6B). But these proteins were mainly histones, most probably due to the contamination from the nucleus. Notably, the M-L subfraction had the highest percentage of TM proteins, among which 102 (46.5%) had at least one transmembrane domain as shown in Figure 6C. This was much higher than that of N-L subfraction (27.9%) and N-H subfraction (27.3%).

According to the cellular component from GO annotation and the literature, 371 (60.5%) proteins were classified as PM or membrane-associated proteins, including 150 (24.5%) from PM annotation, 115 (18.8%) from membrane, 69 (11.3%) from cytoskeleton, and 37 (6.0%) from cytoplasmic locations as shown in Figure 7A. As predicted from TMHMM algorithms, 198 (32.4%) had at least one transmembrane domain. It should be mentioned that the data came from the whole membrane fractions including the soluble fraction after Na_2CO_3 treatment, and the percentage was even higher than the data from several membrane proteomics after enrichment for integral membrane protein [Zhang et al., 2006]. The main potential contaminants were derived from mitochondria (10.8%), nucleus (9.5%), and ER (5.4%). The remainder was 85 (13.9%) from other or unknown locations. When the subfractions were taken into consideration as shown in Figure 7A, the M-L subfraction showed the highest percentage for PM and membrane annotations. The N-H subfraction contained

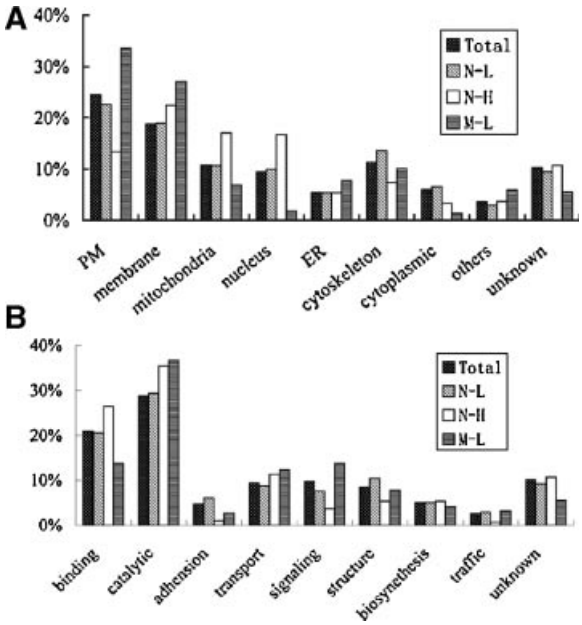

Fig. 7. Functional and subcellular categories of the identified proteins from rat hepatocyte plasma membrane. **A**: The subcellular location categories; (**B**) the functional categories. Total meant all the proteins identified, N-L meant all the proteins identified from the N-L subfractions, N-H meant all the proteins identified from the N-H subfractions, M-L meant all the proteins identified from the M-L subfractioons.

the most contaminants for nucleus and mitochondria, just as the western blotting and the physicochemical performance. The N-L subfraction had a little more percentage proteins from cytoskeleton and cytoplasmic annotations.

The proteins were also categorized according to GO function annotation and reported functions. From Figure 7B, 177 (28.9%) and 128 (20.9%) were catalytic and binding proteins, respectively. The high percentages of these two types might be due to the ambiguous annotation of the GO database. Most interestingly, we identified 60 (9.8%), 58 (9.5%), and 29 (4.7%) from signaling, transporter, adhesion functions, which were very important functional groups known to be especially enriched on liver PM [Evans, 1980]. There were 52 (18.5%) from cell structure and 16 (2.6%) involved in membrane trafficking, functioning in the maintaining the hepatocyte polarity and protein traffic [Wang and Boyer, 2004]. Lastly, 62 (10.1%) of the proteins were yet unknown functional proteins. At the subfraction level in Figure 7B, the M-L subfraction had the highest percentage for signaling, the N-H subfraction showed a little more percentage for biosynthesis and unknown annotations, and the N-L subfraction contained the highest percentage for cell structure.

The overlap of the identified proteins from the three subfractions was indicated in Figure 6A. There were several proteins, found in only one subfraction, which may indicate their potential unique locations. Some of these proteins were reported to be subfraction-specific, such as asialoglycoprotein receptor 2 (IPI00569132), which located on the sinusoidal membrane of hepatocytes where it binds and endocytoses galactose-terminated glycoproteins [Braun et al., 1996], was identified only from the M-L subfraction; desmoplakin, a cell–cell adhesion protein at the surface membrane was only identified from the N-H subfraction. Most of the identified proteins came from at least two subfractions, implicating their multiple locations, but these also may be derived from overlap contaminants. The number of unique peptides identified the proteins were extracted according to different PM subfractions, different sample treatment and separation methods, which were used to analysis the separation and identification details (Supplementary Table S1). At the same time, the emPAI value of all the identified proteins which considered the number of the peptides per protein with the normalization of the theoretical number peptides were calculated in batches and employed as the relative protein abundance [Ishihama et al., 2005]. Due to the relative enrichment of certain subfraction, the resident proteins for certain subfraction would have higher protein abundance than other proteins from contaminations. Then the possible real localization of the identified proteins might be deduced from the emPAI value by the trend analysis [Ong and Mann, 2005; Gilchrist et al., 2006]. This semiquantitative method was verified by several proteins with known subfraction-enriched locations, such as Bile salt export pump (IPI00195615), a canalicular PM protein mediating excretion of bile acids from liver cells into bile, which has an emPAI value of 0.043 from the N-L subfraction and 0.011 from the M-L subfractions; Canalicular multispecific organic anion transporter 1 (IPI00205806), an efflux pump involved in biliary secretion of xenobiotics, was identified with an emPAI value of 0.028 from the N-L subfraction and 0.018 from the M-L subfraction. With this type

of quantitative data, potential information of protein localization was provided for several identified proteins, especially for some novel proteins. In this way, some representative proteins showing location-enriched information were grouped into selected functional categories (Table I), and finally a diagrammatic representation of the functional modules and their subfraction location information in hepatocyte was proposed based on the literatures and our identified results here (Fig. 8). A number of hormones and cations in blood are known to influence liver functions. To be effective, these receptors and signal molecules should be mainly located at the SPM, such as solute carrier organic anion transporter family involved in bile transport, and vasopressin v1b receptor, were only identified from this subfraction. Syndapin iii, is highly conserved src-homology 3 (SH3)-domain-containing proteins which interacts with the large GTPase dynamin and several other proteins and implicates in vesicle trafficking [Kessels and Qualmann, 2004]. Syndapin–dynamin complexes appeared to play an important role in vesicle fission at different donor membranes, including the PM (endocytosis) and Golgi membranes, which was only identified from the M-L subfraction. Pannexin-2, a membrane of the gap junction proteins in cell–cell communication, was only from the N-H subfraction [Barbe et al., 2006]. Radixin is required to maintain apical canalicular membrane structure and function in rat hepatocytes [Wang et al., 2006], which showed the highest abundance in the N-L subfractions. Plakoglobin and beta-catenin plays a dual role as an adhesion molecule in adherens junctions at the PM and as a key intermediate in the canonical wnt signaling pathway [Weerkamp et al., 2006], which was only identified from the N-L subfraction.

DISCUSSION

The main goals of this study were to (i) identify proteins from PM-associated fractions of hepatocytes; (ii) characterize the partial function-related diversified distribution of those proteins; (iii) evaluate two gel-based methods for the separation of integral membrane proteins and the effect of Na_2CO_3 treatment in membrane protein extraction. Our results have provided some clues to these questions.

Plasma Membranes and Cellular Heterogeneity of Liver Tissue

To reduce the bias and misleading conclusions for the presence of contamination from other tissues, cells or organelles, homogenous cell populations will always be a preferred choice in organelle proteomics research. Moreover, Although the non-hepatocytes account for only 8% of the total surface area of parenchymal membranes, they contain 26.5% of all the PM [Blouin et al., 1977]. These data demonstrated that non-hepatocytic organelles could potentially contaminate subcellular fractions used for biochemical studies on liver PM. Recently, many proteomic researches have been performed on whole liver tissue [Fountoulakis and Suter, 2002], or its subcellular organelles [Goldring et al., 2006; Ying et al., 2006], such as mitochondria [Jiang et al., 2004], and PM [Zhang et al., 2005; Lawson et al., 2006]. For single cell types, several proteomic investigations on the whole hepatocytes [Marko-Varga et al., 2003] or their cytosolic [Stevanovic and Bohley, 2001] or secretion proteome [Farkas et al., 2005] have been made, but little work has been done on the PM proteome of hepatocytes. Therefore, in this study, proteomic analysis was performed on PM of freshly isolated hepatocytes. Several hepatocyte-specific proteins were identified from the dataset, such as splice isoform 2 of solute carrier organic anion transporter family, member 1b2 (IPI00231882), which is exclusively expressed in hepatocyte basolateral PM. While biliary duct cell-specific marker cytokeratins 19 (IPI00372924) was not in our dataset, it was identified in our previous research on PM of liver tissue and showed a coverage of 26% [Zhang et al., 2006]. It would generate a great deal of proteins potential exclusively expressed on hepatocyte PM to subtractively compare our data here with the formerly published dataset from the PM of liver tissue [Zhang et al., 2005, 2006, 2007; Cao et al., 2006], although it cannot be used to exclude the existence of a particular protein in liver tissue PM due to the limited sensitivity of the methods and its authentic orientation should be confirmed by other strategies.

Organelle proteomics study usually begins with the isolation of enriched fraction that contains the organelles of interest and the purity is the prerequisite for a successful proteomic analysis. Wisher et al. firstly

TABLE I. Representative Proteins Identified From the Three Subfractions With Putative Functions

Functions examined	IPI number	Protein description	Score[a]	N-L[b]	N-H[b]	M-L[b]
1. SPM						
Recognition, uptake and degradation of metabolites	IPI00231738	Asialoglycoprotein receptor 1	108	0.15 (2)		0.15 (2)
	IPI00569132	Asialoglycoprotein receptor 2	64			0.11 (2)
	IPI00364948	Fatty aldehyde dehydrogenase	387	0.18 (6)	0.06 (2)	0.31 (10)
	IPI00191416	Bile acid CoA ligase	154	0.02 (1)		0.11 (5)
	IPI00197684	Membrane-bound aminopeptidase P	100			0.17 (4)
Signaling	IPI00231134	Guanine nucleotide-binding protein beta subunit 2-like 1	40			0.05 (1)
	IPI00422067	Guanine nucleotide-binding protein beta subunit 4	56			0.04 (1)
	IPI00421897	Ras-related protein Rab-1a	47			0.18 (3)
	IPI00555185	Rab10, member Ras oncogene family	67			0.10 (2)
Cytoskeleton	IPI00197164	Intercellular adhesion molecule-1 precursor	70			0.15 (4)
	IPI00199608	Carcinoembryonic antigen-related cell adhesion molecule, secretedisoform ceacam1a-4c1 precursor	97	0.04 (1)		0.04 (1)
	IPI00199145	Syndapin	49			0.02 (1)
Receptors and binding	IPI00202913	Testis-type galactosyl receptor	64			0.13 (2)
	IPI00195613	Vasopressin v1b receptor	35			0.04 (1)
	IPI00212694	Epidermal growth factor receptor	106			0.03 (3)
	IPI00189766	Progesterone receptor membrane component 1	36			0.07 (1)
	IPI00370607	Similar to transferrin receptor protein 2	68		0.02 (1)	0.02 (1)
Binding of cations	IPI00208061	Sodium/potassium-transporting ATPase beta-3 chain	64			0.11 (2)
	IPI00339124	Sodium/potassium-transporting ATPase beta-1 chain	121			0.11 (3)
	IPI00421888	Annexin A6	472	0.02 (1)		0.13 (8)
	IPI00365929	Thioredoxin domain containing 7	195			0.06 (2)
Effect of toxins	IPI00231638	Glutathione S-transferase alpha 1	59			0.10 (1)
	IPI00209690	Epoxide hydrolase 1	142	0.11 (4)	0.06 (2)	0.24 (8)
	IPI00555299	Paraoxonase 1	130			0.10 (2)
Antigens	IPI00551681	A2Q (fragment)	85	0.04 (1)	0.12 (3)	
	IPI00551594	AK (fragment)	49			0.11 (3)
	IPI00480654	MHC class Ia protein	145	0.04 (1)		0.19 (5)
	IPI00206780	Plasminogen precursor	52			0.02 (1)
	IPI00556921	Cd36 protein	157			0.13 (4)
Transport of metabolites	IPI00202689	Putative integral membrane transport protein	96			0.13 (4)
	IPI00196643	Solute carrier family 2, facilitated glucose transporter, member 2	65	0.05 (1)		0.05 (1)
Bile transporter	IPI00215390	Splice isoform 1 of solute carrier organic anion transporter family, member 1b2	89			0.05 (2)
	IPI00214674	Solute carrier organic anion transporter family, member 1a1	85			0.08 (3)
	IPI00214031	Solute carrier organic anion transporter family, member 1a4	156			0.15 (5)
	IPI00361512	Similar to ATP-binding cassette transporter subfamily member 8a	108			0.02 (2)
Miscellaneous	IPI00476177	Liver regeneration-related protein lrrg03	338			0.32 (9)
2. LPM						
Cytoskeleton	IPI00209113	Myosin heavy chain, non-muscle type a	809	0.10 (19)	0.06 (12)	0.07 (13)
	IPI00189819	Actin, cytoplasmic 1	565	0.65 (12)	0.53 (8)	0.53 (8)
	IPI00372601	Myosin heavy polypeptide 13	44		0.01 (2)	
	IPI00394233	Similar to nebulin-related anchoring protein isoform S	79		0.02 (2)	0.02 (2)
Adhension	IPI00409976	Pannexin-2	39		0.02 (1)	
	IPI00366081	Similar to desmoplakin isoform ii	34		0.004 (1)	
Antigen	IPI00365985	Tumor rejection antigen gp96	437	0.07 (5)	0.21 (11)	0.13 (9)
Receptor and binding	IPI00400568	Splice isoform 1 of peripheral-type benzodiazepine receptor-associated protein 1	35		0.02 (3)	
	IPI00562700	Lipoprotein receptor-related protein	37		0.66 (1)	
Miscellaneous	IPI00464440	Sideroflexin 1	546		0.72 (11)	0.05 (1)
	IPI00390639	Similar to fibronectin leucine rich transmembrane protein1	37		0.02 (1)	
	IPI00373193	Similar To PDZ domain containing 6	64		0.02 (2)	
	IPI00364777	Leucine zipper-EF-hand containing transmembrane protein 1	232	0.03 (2)	0.11 (7)	
	IPI00203528	Predicted: similar to stomatin-like protein 2	170		0.23 (6)	
	IPI00364134	Predicted: similar to nipsnap1 protein	146		0.12 (3)	
	IPI00373089	Protein disulfide-isomerase A5 precursor	94	0.05 (2)	0.08 (3)	
	IPI00421609	Akap18 delta isoform	34		0.07 (2)	
3. CPM						
Bile release	IPI00205806	Canalicular multispecific organic anion transporter 1	76	0.03 (3)		0.02 (2)
	IPI00195615	Bile salt export pump	142	0.04 (4)		0.01 (1)

(*Continued*)

TABLE I. (*Continued*)

Functions examined	IPI number	Protein description	Score[a]	N-L[b]	N-H[b]	M-L[b]
	IPI00563674	Atp-binding cassette, subfamily c (cftr/mrp), member 2	42	0.03 (1)		
	IPI00361513	Similar to ATP-binding cassette transporter subfamily member 9	36	0.03 (3)		
Binding of cations	IPI00208026	Selenium binding protein	66	0.03 (1)		
Signaling	IPI00230862	Aminopeptidase N	366	0.08 (4)		0.33 (16)
	IPI00208422	Dipeptidyl peptidase 4	562	0.12 (4)		0.39 (17)
	IPI00370380	Predicted: similar To Ras Homolog gene family, member T	43	0.02 (1)		
	IPI00391507	Splice isoform 2 of ras GTPase-activating protein syngap	47	0.02 (2)		
Cytoskeleton	IPI00421429	Plakoglobin	394	0.23 (8)		
	IPI00358406	Cadherin-associated protein	486	0.09 (7)		0.05 (4)
	IPI00369635	Radixin	290	0.09 (5)		0.03 (2)
	IPI00325912	Beta-Catenin	64	0.04 (2)		
	IPI00365286	Predicted: Similar To Vinculin	113	0.04 (5)		
Transport of metabolites	IPI00198327	Voltage-dependent anion-selective channel protein 2	219	0.35 (6)	0.11 (2)	
	IPI00562085	Similar to solute carrier family 25, member 5	38	0.17 (3)	0.06 (1)	
Miscellaneous	IPI00359491	Similar To Catns Protein	89	0.04 (3)		
	IPI00382270	Ab1-114	70	0.12 (3)	0.04 (1)	
	IPI00382166	Splice isoform 1 of basigin precursor	96	0.18 (3)		0.18 (3)
	IPI00362153	Similar to bullous pemphigoid antigen 1-b	43	0.003 (3)		

[a]The highest Mascot score for the identified protein.
[b]The emPAI value for the identified protein with the unique MS/MS spectra in the parentheses.

prepared three PM subfractions including N-L, N-H, and M-L from rat liver tissue and the purities were then determined by morphological examination and the activities of marker enzymes. In this study, we modified their procedures and found out that the PM-associated sample preparation has been improved. The obvious evidence is that, the M-L subfraction had almost no contaminations from mitochondria, which have been the major contaminations for N-L and N-H subfraction. Besides, we confirmed that the N-L subfraction was mainly from CPM (as shown from the TEM and anti-5′-Nucleotidase detection), the N-H subfraction was relatively rich in LPM (as shown from the TEM) and the M-L subfraction was mainly composed of SPM (as shown from the TEM and anti-adenylyl cyclases V/VI detection). However, the extent of the overlap could not be determined currently. It maybe that the isolation method based on density centrifugation used here is not specific enough to prevent contaminations from each other. Or the localization of conventional markers for the liver PM is controversial. For instance, histochemical 5′-Nucleotidase at light microscopic level was reportedly concentrated at the bile canaliculus [Wachstein and Meisel, 1957], but EM cytochemistry revealed its presence in the other two surface domains [Farquhar et al., 1974]. Moreover, it had been reported the biochemical marker enzymes of blood-sinusoidal and bile-canalicular were also presented in other subfractions in the previous studies [Wisher and Evans, 1975, 1977; Evans, 1980].

The hepatocyte PM-associated proteome in this study showed that 60.5% of the proteins are putative membrane proteins according to GO annotations and literatures. Others were mainly from mitochondria (10.8%), nucleus (9.5%), and ER (5.4%), which was also found in pervious study [Cao et al., 2006; Zhang et al., 2006]. In this analysis, different level of intercellular organelle contaminations could be detected in the three PM-associated subfraction (Fig. 3B). The possible contaminations may be due to different intercellular organelles closely contacted with or communicate with different functional domains of hepatocyte PM. This may also be from the multiple subcellular localizations of proteins. For example, Loeper et al. examined cytochrome P-450 distributions in human hepatocyte PM using several autoantibodies. The results revealed that the specific content in PM was 9% of that in microsomes. Immunoblots showed the presence of cytochromes P-450 1A2, 2C, 2D6, 2E1, and 3A4 in PM [Loeper et al., 1993], among which cytochromes 1A2, 2C, 2E1 were in our dataset. Kim et al. also suggested that PM lipid rafts might contain oxidation-reduction respiratory chains and ATP synthase complex when they found many mitochondrial proteins in lipid rafts of rat liver PM [Bae et al., 2004; Kim et al., 2006]. However, the probable

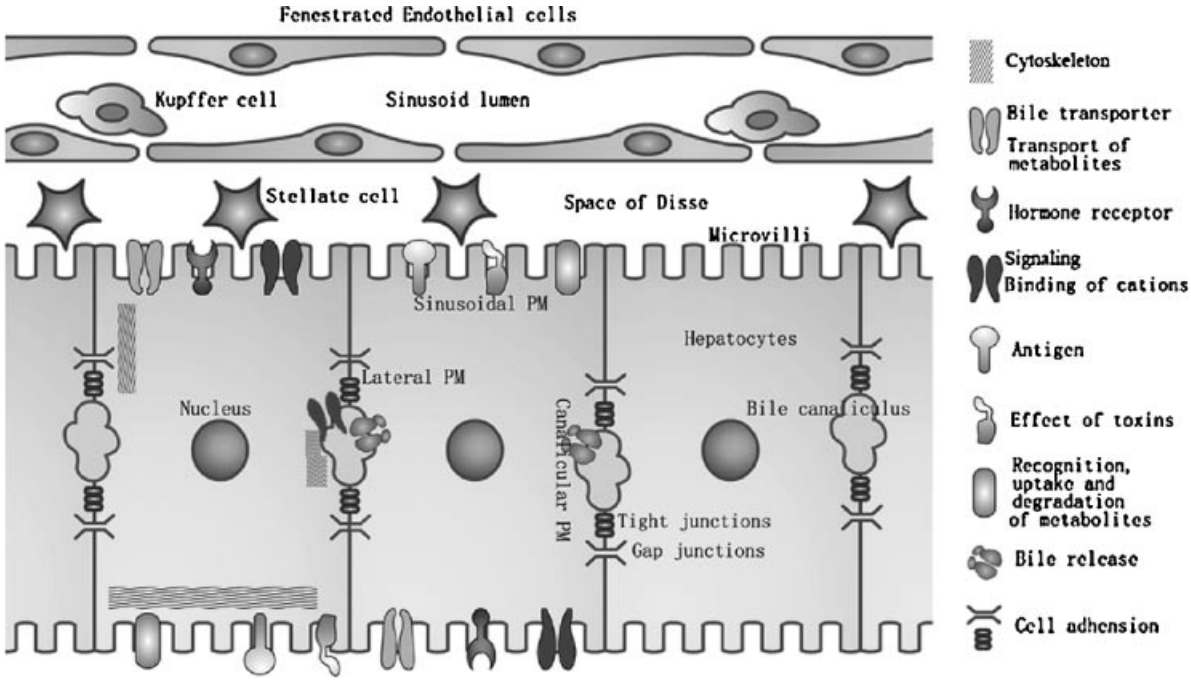

Fig. 8. Diagrammatic representation of the functional modules and their subfraction location information in hepatocytes. The selective proteins of the functional modules were shown in Table I.

contaminations might have resulted from the preparation method based on the densities of the organelles. Other classic cell-biology techniques for isolating PM fractions, such as two-phase partition [Cao et al., 2006] or immunoisolation [Morciano et al., 2005; Lawson et al., 2006; Zhang et al., 2007] could be integrated to get a more purified PM preparations. High-throughput localization of organelle proteins by mass spectrometry, such as protein correlation profiling (PCP) or localization of organelle proteins by isotope tagging (LOPIT), seems to have been an effective strategy to distinguish bona fide organelle proteins from contaminations [Andersen et al., 2003; Dunkley et al., 2004; Goldring et al., 2006]. However, due to the available well-established biochemical methods, the origin complexity of the three subfraction and the uncertainty of the marker proteins for the subfractions, it was not implemented in our research.

Characterization of PM-Associated Proteins From Functional Domains of Hepatocyte

The PM of epithelial cells such as renal epithelial cells and hepatocytes is asymmetrically organized into apical and basolateral regions, which have distinct proteins and lipid compositions. Recently, proteomics strategy has been used to analyze the diversity composition of PM protein on polarized cells successfully [Cutillas et al., 2005; Collins et al., 2006], and many interesting proteins were characterized. Current methods reported for the isolation of liver PM are generally based on separating cell-surface membrane fragments from either the nuclear or microsomal portion of the tissue homogenate. Nevertheless, during the differential centrifugation of live homogenates, certain enzymes exhibited a bimodal distribution between the nuclear and microsomal fractions, and it has been shown that many such enzymes are actual components of the PM. Mazzone et al. [2006] isolated lipid microdomains from apical and basolateral PM of rat hepatocytes successfully, and found that the microdomains were the targets for exocytic insertion and retrieval of "flux proteins," including aquaporin proteins, involved in canalicular bile secretion. However, proteomic analysis of the membrane proteins in the polarized functional domains was not performed.

Subcellular proteomics is able to characterize low abundance proteins as well as provide information on subcellular location. Subcellular structures contain miscellaneous protein complexes, many of which are beyond the sensitivity

of current mass spectrometry-based proteomics. Several biochemical methods, such as chromatography and treatment with chemical regents have been used to prefractionationate a complicated sample. However, during these prefractionation processes, a number of important proteins will be lost to some extent because of the inherent defects of these methods. In this study, whole liver PM was separated into three subfractions according to density heterogeneities and functional diversities, which may synchronously take the advantages of identification of low abundance proteins and preserving sample integrity.

The three subfractions from global liver PM show similar protein composition according to electrophoresis and physicochemical analysis. From the N-L, N-H, and M-L subfractions, 169, 81, and 92 non-redundant proteins, respectively, were uniquely identified (Fig. 6A). Several subfraction-specific proteins were identified in other subfractions due to contamination during sample preparation. This phenomenon was also found in work of Gilchrist et al. [2006]. In their proteomic map of the rough ER, smooth ER, and Golgi apparatus isolated from liver homogenates, they used the redundant peptide counting, another semi-quantitation method, to discriminate the possible contaminations. In our analysis, the semi-quantitation emPAI were employed. A condition applies to this estimation, as extremely abundant proteins may affect the efficiency of protein identification because of ionization suppression and detector saturation of the MS analyzer and/or the detector. Highly hydrophobic proteins may also be under-represented because they generate a limited number of peptides due to their sequence characteristics. Despite these limitations, approximate comparison of the relative abundance of PM proteins is possible because of the common characteristics they share, and this strategy was confirmed by several proteins with known subfraction localization. Through this strategy, the true location could generally be inferred from the emPAI values of these proteins (Supplementary Table I). However, their real locations in the hepatocyte should be examined by other methods, such as immunofluorescence-localization.

Recently published proteome studies on the liver PM were interpreted, the PM of the hepatocyte sinusoidal area mainly from the microsomal fraction were frequently received little attention [Zhang et al., 2005, 2006; Lawson et al., 2006]. Moreover, an estimation of the relative surface area of the three major hepatocyte surface regions is: SPM, 72%; LPM, 15%; and CPM, 13% from a stereological study [Blouin et al., 1977], which was consistent with the yields of our subfraction of 5.7 mg from SPM, 2.5 mg from CPM, and 2.1 mg from LPM per 1 g liver tissue, respectively. Several PM marker proteins had been subsequently identified from the SPM, such as asialoglycoprotein receptor, sodium/potassium-transporting ATPase beta-1 chain and carcinoembryonic antigen-related cell adhesion molecule, further supporting its PM origin. From the subcellular location results, the SPM showed the highest percentage of PM and membrane proteins, and had little contaminant from nucleus and mitochondria, which were consistent with the western blotting results. According to literatures, this subfraction showed the most complicated compositions (Table I), including proteins involved in recognizing, uptaking of metabolites and binding of cations. Many antigens, hormone receptors, and bile transporters were also found in this subfraction. Interestingly, much of the identified proteins might participate in important signaling pathways from the functional catalogues (Fig. 7B). Our dataset has provided a proteomic view of these significant proteins for the first time and would pave the way to understand the functions of the sinusoidal PM.

Additionally, the SPM subfraction has more proteins with transmembrane domains (Fig. 6C). It might give implication to the specific post-Golgi trafficking routines in hepatocyte [Wang and Boyer, 2004], which reveals most canalicular proteins traffic by an indirect route, first to the sinusoidal membrane, followed by transcytosis through basolateral early endosomes and a subapical compartment, before finally targeting to the canalicular domain. To our best knowledge, this was the first report of this phenomenon in a proteomic view. For this unique mechanism, several CPM proteins may be retained at the SPM at the time of our examination. Apart from the contaminant from sample preparation, this might explain why some known CPM marker proteins, such as dipeptidyl peptidase 4 (IPI00208422) and aminopeptidase N (IPI00230862), were also identified in the SPM subfraction. There are several molecular markers involved in hepatocyte polarized transport pathways in our dataset

[Wilton and Matthews, 1996]. Over 30 members of the rab family of GTPases have so far been identified and a number of these have been shown to participate in specific membrane traffic pathways and provide potential targets for therapeutic intervention [Stein et al., 2003]. There are eight such proteins in our dataset (Supplementary Table S1). Efficient targeting of apical membrane proteins relies upon intact microtubules, which extend throughout the hepatocyte cytosol between the basolateral and apical domains [Durand-Schneider et al., 1987]. 12.5% of our identified proteins are from cytoskeleton, such as actin and myosin, and much of these proteins came from the N-L subfraction. In addition, annexin A6 (IPI00421888) has been shown to be associated with traffic endosomes and has been localized to the hepatocyte membrane. The next research target will be to understand the trafficking routes and molecular mechanisms that are used by various canalicular and sinusoidal proteins as they journey along the pathways. Biochemical analysis of proteins in isolated endosomal fractions of liver would provide some clues to this dynamic pathway [Pol et al., 1997].

Due to the higher sucrose density, the LPM subfraction contained higher percentage of proteins from the nucleus and mitochondria. However, this subfraction contained only a few proteins involved in cell junction, such as gap junction and tight junction. This subfraction was enriched in these structures from the TEM results (Fig. 2). The reason may be that much of these proteins were low abundance proteins, which were difficult to be identified in current mass spectrometry-based proteomics, and these proteins always escaped from being identified in other proteomic studies [Foster et al., 2006; Lawson et al., 2006]. The N-L subfraction had the morphologically distinguishable domains from the CPM. Further support for this identification comes from the results of western blotting against 5′-Nucleotidase. The CPM is primarily concerned in secretion of bile and excretion of products detoxicated in the hepatocytes. Several proteins involved in bile release were identified (Table I), such as bile salt export pump (IPI00195615) and canalicular multi-specific organic anion transporter 1 (IPI00205806). However, this subfraction is also contaminated from the SPM as shown from the western blotting again Na^+-K^+ ATPase and identified proteins.

In addition to identify multiple known PM proteins, database searching revealed several proteins with unknown localization or functions. This group includes proteins discovered through EST and cDNA cloning initiatives. We examined these proteins by analyzing the sequences with pfam algorithms (http://www.sanger.ac.uk/software/pfam/index) and the BLAST (basic local alignment search tool) algorithm to evaluate their putative localizations and probable function [Bateman et al., 2002]. For example, hypothetical protein xp_579394 (IPI00563815) with predicted OATP (organic anion transporting polypeptide) domain, may have significant roles involved in bile transport [Mikkaichi et al., 2004]. Similar to PDZ domain containing 6 (IPI00373193) having PDZ (PSD-95/DLG/ZO-1) domain, identified only from the LPM fractions may play a vital role in cell–cell adhesion [Vinken et al., 2006].

Evaluation of the Prefractionation and Separation Methods for Membrane Proteins

Alkaline buffer is known not only to depolymerize actin bundles but also to disrupt noncovalent protein–protein interactions while retaining the association of integral membrane proteins with the lipid bilayer. To examine the real effect and evaluate the experiment condition, both the supernatant and the pellet were analyzed using electrophoresis and mass spectrometry, and the data indicated that Na_2CO_3 treatment was useful in membrane proteins prefractionation (Fig. 4A,B). Nevertheless, the supernatant still has a high percentage of integral membrane proteins (24.3%) and has several proteins with high TM sequences (up to 12). As 47 (71.2%) integral membrane proteins from the supernatant fraction were also identified in the pellet, and 35 (74.5%) had more unique peptides from the pellet fraction than that from the supernatant (Supplementary Table S1). Therefore, this may be due to the incomplete sedimentation of membrane vesicles for the centrifugation force used (18,000*g*) after Na_2CO_3 treatment, which has been used in many such studies [Millar and Heazlewood, 2003; Marmagne et al., 2004; Zhang et al., 2005, 2006]. If the same experiment condition was used, in our opinion, both the supernatant and the pellet should be analyzed in membrane proteomic research to obtain a more comprehensive inventory.

Besides the low abundance of the membrane proteins, the analysis is also challenging due to their hydrophobicity. 1-D SDS–PAGE and 16-BAC/SDS–PAGE are frequently used methods to resolve integral membrane proteins based on gels [Burre et al., 2007]. Not much work has been done to compare these separation methods comprehensively, especially from large-scale identified proteins. From our results, 16-BAC/SDS–PAGE was an alternative strategy to separate integral membrane proteins even with high transmembrane domains (up to 14), and had the advantages of increased resolution, although the high MW proteins (above 200 kDa) were always lost. However, 1-D SDS–PAGE can cover this range. Therefore, the co-operation of these two separation methods could provide complementary information in membrane proteomics research.

In summary, our research reveals that the supernatant from the Na_2CO_3 treatment is the same as important as the pellet for achieving a comprehensive understanding of the membrane proteome. Our results also indicate that the 16-BAC/SDS–PAGE and 1-D SDS–PAGE were complementary method in membrane protein separation. To the best of our knowledge, we have constructed for the first time an initial database of PM-associated proteome of hepatocytes with partial functional domain information and provided the relatively high coverage of protein composition from the sinusoidal PM of hepatocyte. Analysis and comparison of the proteome of three subfractions will give some clues to the generation and maintenance of hepatocyte PM polarity, and will generate novel insight into liver function and membrane dynamics.

ACKNOWLEDGMENTS

We thank Professor Dongyi Zhang for expert technical assistance. We are also grateful to Dr. Ying Wang for good suggestions on the manuscript.

REFERENCES

Andersen JS, Wilkinson CJ, Mayor T, Mortensen P, Nigg EA, Mann M. 2003. Proteomic characterization of the human centrosome by protein correlation profiling. Nature 426:570–574.

Aronson NN, Jr., Touster O. 1974. Isolation of rat liver plasma membrane fragments in isotonic sucrose. Methods Enzymol 31:90–102.

Bae TJ, Kim MS, Kim JW, Kim BW, Choo HJ, Lee JW, Kim KB, Lee CS, Kim JH, Chang SY, Kang CY, Lee SW, Ko YG. 2004. Lipid raft proteome reveals ATP synthase complex in the cell surface. Proteomics 4:3536–3548.

Barbe MT, Monyer H, Bruzzone R. 2006. Cell–cell communication beyond connexins: The pannexin channels. Physiology (Bethesda) 21:103–114.

Bateman A, Birney E, Cerruti L, Durbin R, Etwiller L, Eddy SR, Griffiths-Jones S, Howe KL, Marshall M, Sonnhammer EL. 2002. The Pfam protein families database. Nucleic Acids Res 30:276–280.

Blouin A, Bolender RP, Weibel ER. 1977. Distribution of organelles and membranes between hepatocytes and nonhepatocytes in the rat liver parenchyma. A stereological study. J Cell Biol 72:441–455.

Braun JR, Willnow TE, Ishibashi S, Ashwell G, Herz J. 1996. The major subunit of the asialoglycoprotein receptor is expressed on the hepatocellular surface in mice lacking the minor receptor subunit. J Biol Chem 271:21160–21166.

Burre J, Zimmermann H, Volknandt W. 2007. Immunoisolation and subfractionation of synaptic vesicle proteins. Anal Biochem 362:172–181.

Cao R, Li X, Liu Z, Peng X, Hu W, Wang X, Chen P, Xie J, Liang S. 2006. Integration of a two-phase partition method into proteomics research on rat liver plasma membrane proteins. J Proteome Res 5:634–642.

Chen P, Li X, Sun Y, Liu Z, Cao R, He Q, Wang M, Xiong J, Xie J, Wang X, Liang S. 2006. Proteomic analysis of rat hippocampal plasma membrane: Characterization of potential neuronal-specific plasma membrane proteins. J Neurochem 98:1126–1140.

Collins MO, Husi H, Yu L, Brandon JM, Anderson CN, Blackstock WP, Choudhary JS, Grant SG. 2006. Molecular characterization and comparison of the components and multiprotein complexes in the postsynaptic proteome. J Neurochem 97 (Suppl 1):16–23.

Cutillas PR, Biber J, Marks J, Jacob R, Stieger B, Cramer R, Waterfield M, Burlingame AL, Unwin RJ. 2005. Proteomic analysis of plasma membrane vesicles isolated from the rat renal cortex. Proteomics 5:101–112.

Dunkley TP, Watson R, Griffin JL, Dupree P, Lilley KS. 2004. Localization of organelle proteins by isotope tagging (LOPIT). Mol Cell Proteomics 3:1128–1134.

Durand-Schneider AM, Maurice M, Dumont M, Feldmann G. 1987. Effect of colchicine and phalloidin on the distribution of three plasma membrane antigens in rat hepatocytes: Comparison with bile duct ligation. Hepatology 7:1239–1248.

Durr E, Yu J, Krasinska KM, Carver LA, Yates JR, Testa JE, Oh P, Schnitzer JE. 2004. Direct proteomic mapping of the lung microvascular endothelial cell surface in vivo and in cell culture. Nat Biotechnol 22: 985–992.

Enrich C, Tabona P, Evans WH. 1990. A two-dimensional electrophoretic analysis of the proteins and glycoproteins of liver plasma membrane domains and endosomes. Implications for endocytosis and transcytosis. Biochem J 271:171–178.

Evans WH. 1980. A biochemical dissection of the functional polarity of the plasma membrane of the hepatocyte. Biochim Biophys Acta 604:27–64.

Farkas D, Bhat VB, Mandapati S, Wishnok JS, Tannenbaum SR. 2005. Characterization of the secreted proteome of rat hepatocytes cultured in collagen sandwiches. Chem Res Toxicol 18:1132–1139.

Farquhar MG, Bergeron JJ, Palade GE. 1974. Cytochemistry of Golgi fractions prepared from rat liver. J Cell Biol 60:8–25.

Fleischer S, Kervina M. 1974. Subcellular fractionation of rat liver. Methods Enzymol 31:6–41.

Foster LJ, de Hoog CL, Zhang Y, Zhang Y, Xie X, Mootha VK, Mann M. 2006. A mammalian organelle map by protein correlation profiling. Cell 125:187–199.

Fountoulakis M, Suter L. 2002. Proteomic analysis of the rat liver. J Chromatogr B Analyt Technol Biomed Life Sci 782:197–218.

Gilchrist A, Au CE, Hiding J, Bell AW, Fernandez-Rodriguez J, Lesimple S, Nagaya H, Roy L, Gosline SJ, Hallett M, Paiement J, Kearney RE, Nilsson T, Bergeron JJ. 2006. Quantitative proteomics analysis of the secretory pathway. Cell 127:1265–1281.

Goldring CE, Kitteringham NR, Jenkins R, Lovatt CA, Randle LE, Abdullah A, Owen A, Liu X, Butler PJ, Williams DP, Metcalfe P, Berens C, Hillen W, Foster B, Simpson A, McLellan L, Park BK. 2006. Development of a transactivator in hepatoma cells that allows expression of phase I, phase II, and chemical defense genes. Am J Physiol Cell Physiol 290:C104–C115.

Hartinger J, Stenius K, Hogemann D, Jahn R. 1996. 16-BAC/SDS–PAGE: A two-dimensional gel electrophoresis system suitable for the separation of integral membrane proteins. Anal Biochem 240:126–133.

Hubbard AL, Wall DA, Ma A. 1983. Isolation of rat hepatocyte plasma membranes. I. Presence of the three major domains. J Cell Biol 96:217–229.

Ishihama Y, Oda Y, Tabata T, Sato T, Nagasu T, Rappsilber J, Mann M. 2005. Exponentially modified protein abundance index (emPAI) for estimation of absolute protein amount in proteomics by the number of sequenced peptides per protein. Mol Cell Proteomics 4:1265–1272.

Jiang XS, Zhou H, Zhang L, Sheng QH, Li SJ, Li L, Hao P, Li YX, Xia QC, Wu JR, Zeng R. 2004. A high-throughput approach for subcellular proteome: Identification of rat liver proteins using subcellular fractionation coupled with two-dimensional liquid chromatography tandem mass spectrometry and bioinformatic analysis. Mol Cell Proteomics 3:441–455.

Josic D, Clifton JG. 2007. Mammalian plasma membrane proteomics. Proteomics 6:3614–3627.

Kessels MM, Qualmann B. 2004. The syndapin protein family: Linking membrane trafficking with the cytoskeleton. J Cell Sci 117:3077–3086.

Kim KB, Lee JW, Lee CS, Kim BW, Choo HJ, Jung SY, Chi SG, Yoon YS, Yoon G, Ko YG. 2006. Oxidation-reduction respiratory chains and ATP synthase complex are localized in detergent-resistant lipid rafts. Proteomics 6:2444–2453.

Lawson EL, Clifton JG, Huang F, Li X, Hixson DC, Josic D. 2006. Use of magnetic beads with immobilized monoclonal antibodies for isolation of highly pure plasma membranes. Electrophoresis 27:2747–2758.

Loeper J, Descatoire V, Maurice M, Beaune P, Belghiti J, Houssin D, Ballet F, Feldmann G, Guengerich FP, Pessayre D. 1993. Cytochromes P-450 in human hepatocyte plasma membrane: Recognition by several autoantibodies. Gastroenterology 104:203–216.

Marko-Varga G, Berglund M, Malmstrom J, Lindberg H, Fehniger TE. 2003. Targeting hepatocytes from liver tissue by laser capture microdissection and proteomics expression profiling. Electrophoresis 24:3800–3805.

Marmagne A, Rouet MA, Ferro M, Rolland N, Alcon C, Joyard J, Garin J, Barbier-Brygoo H, Ephritikhine G. 2004. Identification of new intrinsic proteins in Arabidopsis plasma membrane proteome. Mol Cell Proteomics 3:675–691.

Mazzone A, Tietz P, Jefferson J, Pagano R, LaRusso NF. 2006. Isolation and characterization of lipid microdomains from apical and basolateral plasma membranes of rat hepatocytes. Hepatology 43:287–296.

Mikkaichi T, Suzuki T, Tanemoto M, Ito S, Abe T. 2004. The organic anion transporter (OATP) family. Drug Metab Pharmacokinet 19:171–179.

Millar AH, Heazlewood JL. 2003. Genomic and proteomic analysis of mitochondrial carrier proteins in Arabidopsis. Plant Physiol 131:443–453.

Morciano M, Burre J, Corvey C, Karas M, Zimmermann H, Volknandt W. 2005. Immunoisolation of two synaptic vesicle pools from synaptosomes: A proteomics analysis. J Neurochem 95:1732–1745.

Ong SE, Mann M. 2005. Mass spectrometry-based proteomics turns quantitative. Nat Chem Biol 1:252–262.

Pol A, Ortega D, Enrich C. 1997. Identification and distribution of proteins in isolated endosomal fractions of rat liver: Involvement in endocytosis, recycling and transcytosis. Biochem J 323(Pt 2):435–443.

Seglen PO. 1976. Preparation of isolated rat liver cells. Methods Cell Biol 13:29–83.

Stein MP, Dong J, Wandinger-Ness A. 2003. Rab proteins and endocytic trafficking: Potential targets for therapeutic intervention. Adv Drug Deliv Rev 55:1421–1437.

Stevanovic S, Bohley P. 2001. Proteome analysis by three-dimensional protein separation: Turnover of cytosolic proteins in hepatocytes. Biol Chem 382:677–682.

Tennant JR. 1964. Evaluation of the trypan blue technique for determination of cell viability. Transplantation 2:685–694.

Torok K, Stauffer K, Evans WH. 1997. Connexin 32 of gap junctions contains two cytoplasmic calmodulin-binding domains. Biochem J 326(Pt 2):479–483.

Vinken M, Papeleu P, Snykers S, De Rop E, Henkens T, Chipman JK, Rogiers V, Vanhaecke T. 2006. Involvement of cell junctions in hepatocyte culture functionality. Crit Rev Toxicol 36:299–318.

Wachstein M, Meisel E. 1957. Histochemistry of hepatic phosphatases of a physiologic pH; with special reference to the demonstration of bile canaliculi. Am J Clin Pathol 27:13–23.

Wang L, Boyer JL. 2004. The maintenance and generation of membrane polarity in hepatocytes. Hepatology 39:892–899.

Wang W, Soroka CJ, Mennone A, Rahner C, Harry K, Pypaert M, Boyer JL. 2006. Radixin is required to maintain apical canalicular membrane structure and function in rat hepatocytes. Gastroenterology 131:878–884.

Weerkamp F, Baert MR, Naber BA, Koster EE, de Haas EF, Atkuri KR, van Dongen JJ, Herzenberg LA, Staal FJ. 2006. Wnt signaling in the thymus is regulated by differential expression of intracellular signaling molecules. Proc Natl Acad Sci USA 103:3322–3326.

Wilton JC, Matthews GM. 1996. Polarised membrane traffic in hepatocytes. Bioessays 18:229–236.

Wisher MH, Evans WH. 1975. Functional polarity of the rat hepatocyte surface membrane. Isolation and characterization of plasma-membrane subfractions from the blood-sinusoidal, bile-Canalicular and contiguous surfaces of the hepatocyte. Biochem J 146:375–388.

Wisher MH, Evans WH. 1977. Preparation of plasma-membrane subfractions from isolated rat hepatocytes. Biochem J 164:415–422.

Wu CC, Yates JR III. 2003. The application of mass spectrometry to membrane proteomics. Nat Biotechnol 21:262–267.

Yates JR III, Gilchrist A, Howell KE, Bergeron JJ. 2005. Proteomics of organelles and large cellular structures. Nat Rev Mol Cell Biol 6:702–714.

Ying W, Jiang Y, Guo L, Hao Y, Zhang Y, Wu S, Zhong F, Wang J, Shi R, Li D, Wan P, Li X, Wei H, Li J, Wang Z, Xue X, Cai Y, Zhu Y, Qian X, He F. 2006. A dataset of human fetal liver proteome identified by subcellular fractionation and multiple protein separation and identification technology. Mol Cell Proteomics 5:1703–1707.

Zhang L, Xie J, Wang X, Liu X, Tang X, Cao R, Hu W, Nie S, Fan C, Liang S. 2005. Proteomic analysis of mouse liver plasma membrane: Use of differential extraction to enrich hydrophobic membrane proteins. Proteomics 5:4510–4524.

Zhang LJ, Wang XE, Peng X, Wei YJ, Cao R, Liu Z, Xiong JX, Yin XF, Ping C, Liang S. 2006. Proteomic analysis of low-abundant integral plasma membrane proteins based on gels. Cell Mol Life Sci 63:1790–1804.

Zhang L, Wang X, Peng X, Wei Y, Cao R, Liu Z, Xiong J, Ying X, Chen P, Liang S. 2007. Immunoaffinity purification of plasma membrane with secondary antibody superparamagnetic beads for proteomic analysis. J Proteome Res 6:34–43.